5 (2026) 100283

Contents lists available at ScienceDirect

Journal of Subatomic Particles and Cosmology

journal homepage: https://www.sciencedirect.com/journal/journal-of-subatomic-particles-and-cosmology

Full Length Article

QCD Transition line up to $\mu_B = 400$ MeV from finite volume lattice simulations

Szabolcs Borsányi [a], Zoltán Fodor [b,c,a,d,e], Jana N. Guenther [a], Paolo Parotto [f], Attila Pásztor [d,g], Ludovica Pirelli [a,*], Kálmán K. Szabó [a,e], Chik Him Wong [a]

[a] Wuppertal University, Gaussstr. 20, Wuppertal, 42119, Germany
[b] Pennsylvania State University, 16801, State College, PA, USA
[c] Institute for Computational and Data Sciences, Pennsylvania State University, 16802, University Park, PA, USA
[d] Institute for Theoretical Physics, ELTE Eötvös Loránd University, Pázmány P. sétány 1/A, H-1117, Budapest, Hungary
[e] Jülich Supercomputing Centre, Jülich, Jülich, D-52425, Germany
[f] Università di Torino and INFN Torino, Via P. Giuria 1, I-10125, Torino, Italy
[g] MTA-ELTE Lendület "Momentum" Strongly Interacting Matter Research Group, Pázmány P. sétány 1/A, H-1117, Budapest, Hungary

ARTICLE INFO

Keywords:
Lattice QCD
Phase diagram
CEP

ABSTRACT

A standard way to compute the QCD crossover line in the temperature (T) - baryochemical potential (μ_B) plane with lattice techniques is to extract it from the chiral condensate or from the peak position of the chiral susceptibility. However, these quantities suffer from not-negligible volume effects, as shown in [1]. Here we draw the QCD crossover line from the peak position of an alternative observable, the static quark entropy ($S_Q(T,\mu_B)$), based on the renormalized Polyakov loop, that was shown to have a peak in the vicinity of the chiral transition temperature in [2]. The advantage is that it has smaller volume effects. That allow us to extrapolate $S_Q(T,\mu_B)$ by means of a Taylor expansion to eighth order in μ_B(NNNLO) on a 16×8 lattice. We use high-statistics simulations with 2+1 4HEX staggered fermions at physical quark masses. The results are computed along the strangeness neutral line. We are able to draw the phase diagram up to $\mu_B \approx 400$ MeV, finding a rough agreement with phenomenological estimates of the freeze-out curve in relativistic heavy ion collisions. We see that the width of the crossover increases at higher densities, disfavoring the existence of a critical endpoint in the explored range.

1. Introduction

An important line of research in QCD under extreme conditions of temperature and baryon density is the determination of the transition line in the $T - \mu_B$ phase diagram. Direct lattice QCD calculations have been hampered by the well known sign problem. Among the techniques that are used to circumvent it we find Taylor methods, so by computing the desired observables at finite μ_B as a Taylor expansion around $\mu_B = 0$. Since the simulation are performed only at $\mu_B = 0$, there is no complex action problem, however some residual effects still manifest as strong cancellations inside the derivatives. We show that for the baryon number fluctuations, that are μ_B-derivatives of the pressure:

$$\chi_n = \left(\frac{\partial^n (p/T^4)}{\partial(\mu_B/T)^n}\right)_{\mu_B=0}. \tag{1}$$

In Fig. 1 we see that there is an almost equal number of positive and negative terms contributing to each χ_n, making the computation increasingly difficult as n increases. However, the cancellation problem is less severe for smaller volumes, hence our use of a $16^3\times 8$ lattice. This problem was discussed also in [3]. We so need to investigate which observable can provide a better proxy for the transition line even at small volumes: such an investigation was done in detail in [1]. Typical observables to study the crossover line are the chiral condensate, that is an order parameter for chiral symmetry in the limit of zero light quark masses, and the chiral susceptibility. A crossover line extrapolated from the peak of the chiral susceptibility was drawn up to $\mu_B \approx 300$ MeV in [4]. However, as shown in [1], these observables have not negligible volume effects. We then follow an idea that was suggested in [2]: we use the peak of the static quark entropy, a Polyakov loop derived observable, as a proxy for the crossover line. This observable has smaller volume effects, hence we expect to be able to use Taylor methods up to high orders. In the results Section 4 we draw the crossover line from the peak of the static quark entropy up to $\mu_B \approx 400$ MeV. We compute the Polyakov loop derivatives up to eight order and from that we compute

* Corresponding author.
E-mail address: pirelli@uni-wuppertal.de (L. Pirelli).

https://doi.org/10.1016/j.jspc.2025.100283
Received 25 November 2025; Received in revised form 18 December 2025; Accepted 18 December 2025
Available online 24 December 2025

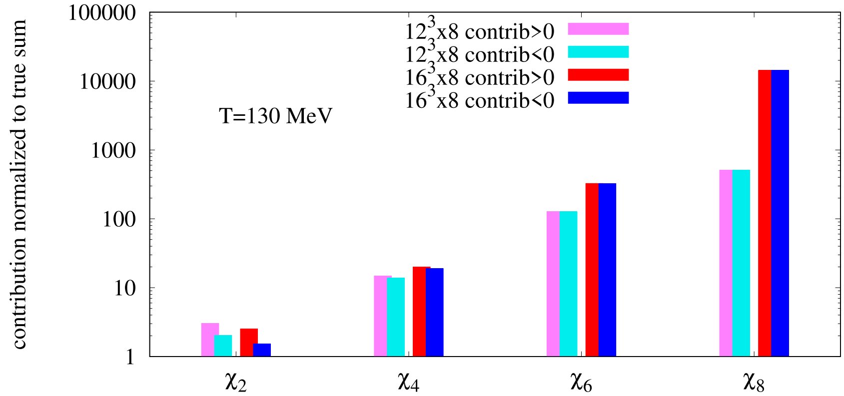

Fig. 1. Cancellations between positive and negative terms for the Taylor coefficients χ_n for up to the eighth order at $T = 130$ MeV. Positive contributions are shown in red, while negative contributions are shown in blue. A smaller volume ($12^3 \times 8$) is also shown, to illustrate the volume dependence of the cancellations. (For interpretation of the references to colour in this figure legend, the reader is referred to the web version of this article.)

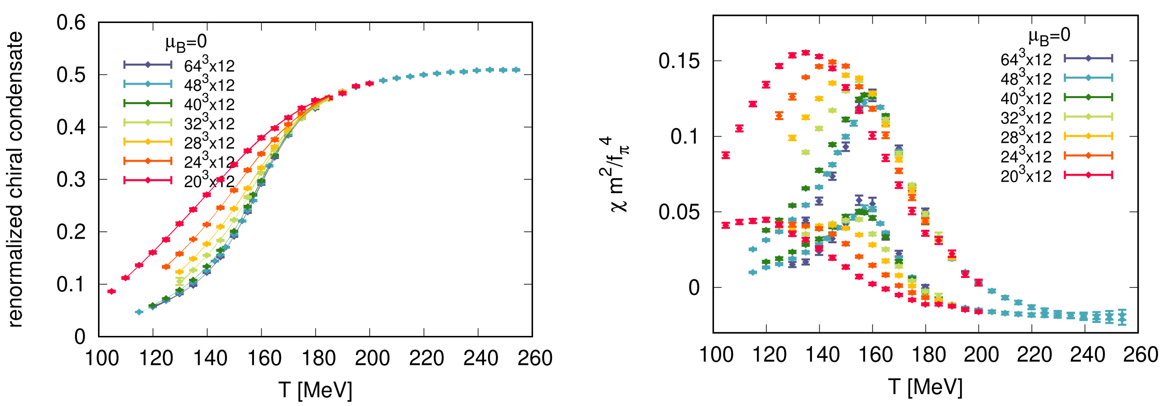

Fig. 2. Left panel: The renormalized chiral condensate (see Eq. (4)) as a function of temperature for different volumes, at $\mu_B = 0$. Right panel: The renormalized full and disconnected chiral susceptibility as a function of temperature for different volumes at $\mu_B = 0$.

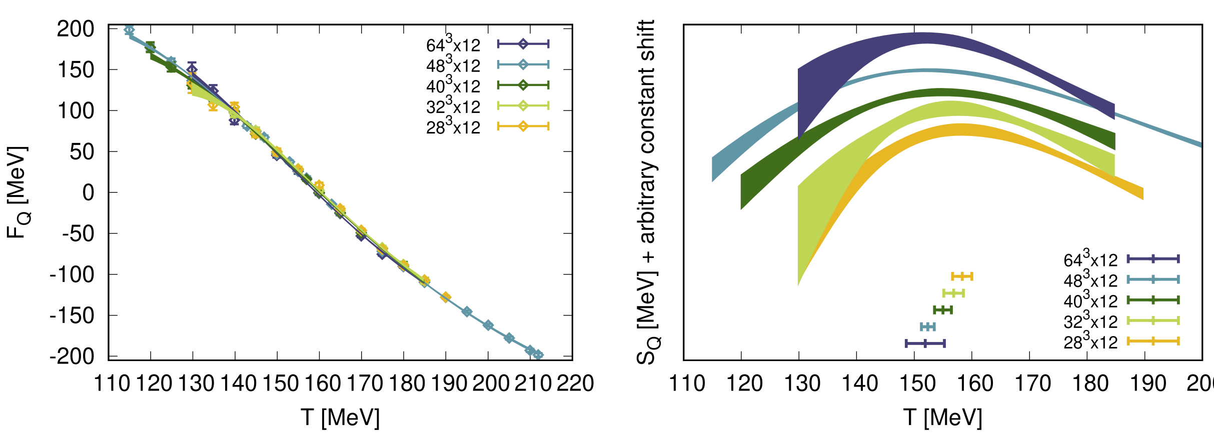

Fig. 3. Left panel: The static quark free energy (see Eq. (6)) as a function of temperature for different volumes, at $\mu_B = 0$. Right panel: The static quark entropy as a function of temperature for different volumes, at $\mu_B = 0$. In order for the curves not to overlap, they were shifted by arbitrary amounts in the vertical direction.

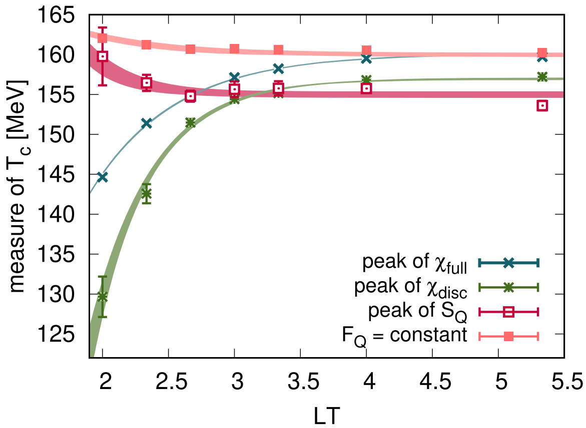

Fig. 4. Five different definitions of the transition temperature as functions of the simulation volume, labeled by the aspect ratio $LT = N_x/N_t$.

the static quark entropy. Our results for the Polyakov loop from the Taylor expansion are crosschecked with results at imaginary μ_B simulations. We also check the robustness of the Taylor expansion by comparing different orders. From the static quark entropy we extract both the peak position, to draw the crossover line, as well as the width of the curves, that give information on the width of the transition, analogously to what happens for the chiral susceptibility in [4]. We see that the transition width tends to increase in the computing range, leading to the conclusion that we do not find evidence of a critical endpoint (CEP) up to $\mu_B \approx 400$ MeV.

2. Volume effects

Observables that are strictly related to the chiral aspects of the QCD crossover are the chiral condensate $\langle\bar\psi\psi\rangle$ and the chiral susceptibility (disconnected, $\chi_{\rm disc}$ and not, χ), that have respectively an inflection point and a peak in the vicinity of the crossover:

$$\langle\bar\psi\psi\rangle = \frac{T}{V}\frac{\partial \log Z}{\partial m_{ud}}, \qquad \chi = \frac{T}{V}\frac{\partial^2 \log Z}{\partial m_{ud}^2}, \tag{2}$$

$$\chi_{\rm disc} = \frac{T}{V}\left(\frac{\partial^2}{\partial m_u \partial m_d}\log Z\right)_{m_u=m_d}, \tag{3}$$

They are renormalized as follows:

$$\begin{aligned}\langle\bar\psi\psi\rangle^R &= -\frac{m_{ud}}{f_\pi^4}\left[\langle\bar\psi\psi\rangle_T - \langle\bar\psi\psi\rangle_{T=0}\right],\\ \chi^R &= \frac{m_{ud}^2}{f_\pi^4}\left[\chi_T - \chi_{T=0}\right].\\ \chi^R_{\rm disc} &= \frac{m_{ud}^2}{f_\pi^4}\left[\chi_{\rm disc,T} - \chi_{\rm disc,T=0}\right],\end{aligned} \tag{4}$$

Their volume effects are visible in Fig. 2, where the chiral condensate and the chiral susceptibilities are at $\mu_B = 0$ for different volumes. From the plot it is clear that T_c changes with the volume.

In Ref. [2] a different observable was proposed to estimate the crossover line. The starting point is the Polyakov loop

$$P = \frac{1}{3}\frac{1}{V}\left\langle \sum_{\vec{x}\in V} \mathrm{Tr} \prod_{t=0}^{N_t-1} U_0(t,\vec{x})\right\rangle, \tag{5}$$

that is an order parameter for deconfinement in the quenched theory. It is, however, not practical to study, since it requires a scheme-dependent multiplicative renormalization. The static quark free energy, instead,

$$F_Q = -T\log P, \tag{6}$$

requires additive renormalization and does not suffer from such an ambiguity. In Ref. [2] its temperature derivative, the static quark free energy, was examined

$$S_Q(T,\mu_B) = -\frac{\partial F_Q(T,\mu_B)}{\partial T}, \tag{7}$$

finding that $S_Q(T,\mu_B)$ has a peak exactly in the vicinity of the chiral crossover. That holds for different values of the quark masses, including the physical values, making the peak position of $S_Q(T,\mu_B)$ a possible proxy to study the transition line. It has also smaller volume effects with respect to the chiral condensate and the susceptibilities, as we can see from Fig. 3: $F_Q(T,0)$ and $S_Q(T,0)$ are plotted for different volumes as in Fig. 2, but in this case the different curves overlap.

A final comparison of the volume effects in the estimation of T_c from different observables is shown in Fig. 4, where it is evident that the crossover temperature estimated from the peak position of S_Q is less volume-dependant as that from the peak position of the chiral susceptibilities.

3. Lattice setup

In the following we show results computed with 2+1 flavors at physical quark masses, on a $16^3\times 8$ lattice. We used a 4HEX staggered fermionic action in the simulations ([6,7]).

4. Crossover line from S_Q peak

The starting point for the computation are the Polyakov loop derivatives, that are computed up to the eight order.

This allows to compute the derivatives of the static quark free energy F_n, from which we can compute

$$\begin{aligned}F_Q(T,\mu_B) &= -\frac{T}{2}\log|\langle P\rangle|^2 =\\ &= F_Q(T,\mu_B=0) + T\sum_{n=2,4,\dots}\frac{F_n}{n!}\left(\frac{\mu_B}{T}\right)^n,\end{aligned} \tag{8}$$

and then derive for each μ_B the static quark entropy S_Q as a T-derivative (Eq. (7)). More details on the computation can be found in [5]; here we discuss only briefly the results and their robustness.

To check the convergence of the Taylor series, we make a crosscheck at imaginary μ_B, where results from direct simulations are available (Fig. 5). We see that the higher orders tend to converge to the direct results. We then go to real μ_B and plot the renormalized Polyakov loop and static quark entropy (Fig. 6).

The Polyakov loop is plotted as a function of μ_B for different temperatures; for $T = 130$ MeV the fourth, sixth and Taylor orders are shown. The eight order starts to deviate from the sixth order around $\mu_B \sim 400$ MeV. The static quark entropy is plotted as a function of T for different μ_B, including a curve obtained at imaginary μ_B. We see that the peaks become wider and lower as μ_B increases, while we would expect them to become narrower and higher in the vicinity of a criticality. At $\mu_B \sim 400$ it is visibly difficult to extract a peak from S_Q. That hints for an absence of a critical end point in this μ_B range.

To confirm our results until $\mu_B \approx 400$ MeV we make a final check on the convergence of the Taylor series. We draw the crossover line from the peak position of S_Q, computed up to the sixth or the eight order (Fig. 7). We also do that in two different setups: in a strangeness neutral setup ($n_S = 0$) or at zero strangeness chemical potential ($\mu_S = 0$). While the latter is technically easier, the first is phenomenologically more interesting, since it respects the same conditions as in heavy-ions collisions, and it is then our priviliged setup. We see that the eight order starts to add a contribution only at $\mu_B \approx 300$ MeV and that the sixth and the eight order are still compatible within errors until $\mu_B \approx 400$ MeV. We can then safely draw our crossover line until $\mu_B \approx 400$ MeV.

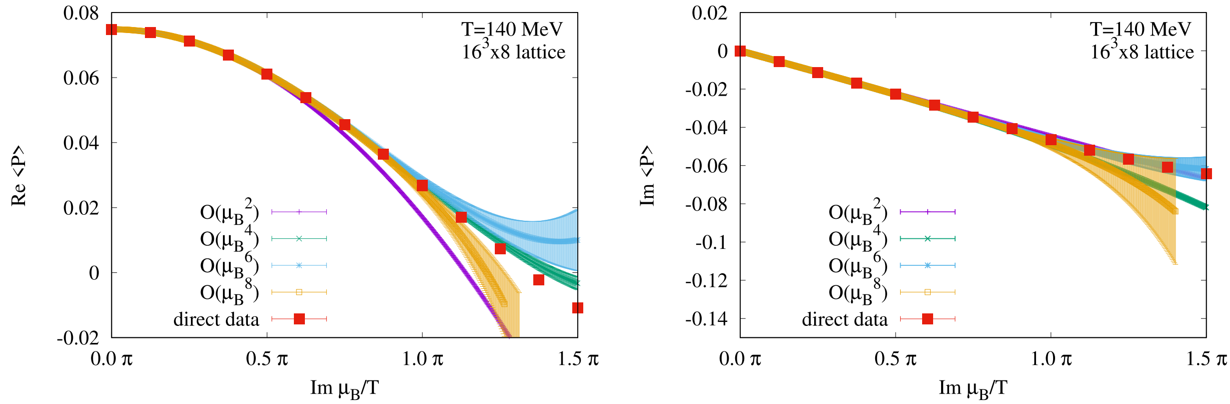

Fig. 5. Check of the convergence of the series: at $T = 140$ MeV, we compare the results from the Taylor series at different orders with results directly measured expectation values at Im $\mu_B > 0$ from a separate set of simulations.

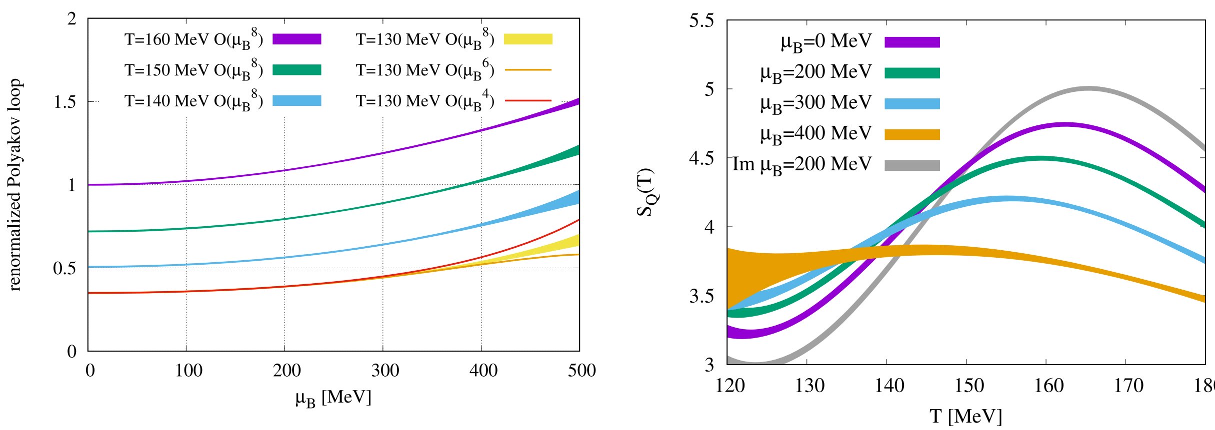

Fig. 6. Left: Renormalized Polyakov loop (P^r) as a function of the μ_B for various temperatures. Right: The static quark entropy ($S_Q(T)$) extrapolated to various chemical potentials. We added the result with an imaginary chemical potential for comparison (gray line).

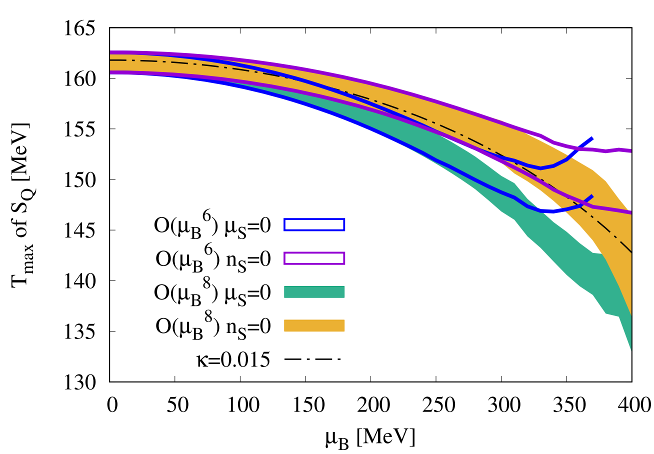

Fig. 7. The maximum position of $S_Q(T)$ for fixed baryo-chemical potential (μ_B), with ($n_S = 0$) and without ($\mu_S = 0$) strangeness neutrality, up to the sixth and up to the eight order in the Taylor expansion.

The final result is shown in Fig. 8. We show our crossover line, compared to the one obtained in Ref. [4], to Dyson-Schwinger based results (Ref. [8]) and to the chemical freezeout datas (Refs. [9,10]). We also show the transition width from [4] and the transition width defined from S_Q as

$$\Delta T(\mu_B) = \sqrt{-S_Q(T,\mu_B) \Big/ \frac{\partial^2 S_Q(T,\mu_B)}{\partial T^2}}\Bigg|_{T=T_c(\mu_B)} \tag{9}$$

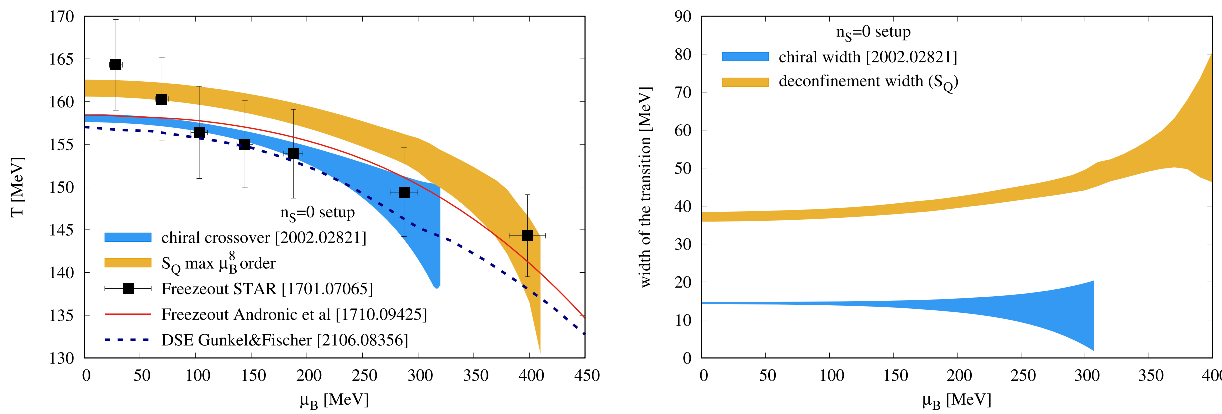

Fig. 8. Left: Crossover (orange) defined as the peak position of the static quark entropy (S_Q) at fixed μ_B as a function of μ_B. We add the chiral transition line from lattice QCD [4] in the phase diagram, defined from the peak of the full chiral susceptibility, as well as the corresponding result based on Dyson-Schwinger equations [8] (the latter used the $\mu_S = \mu_B/3$ scheme as an approximation to $n_S = 0$). We also include the chemical freeze-out parameters [9,10]. Right: the corresponding widths.

As hinted from Fig. 6, we see a broadening of the transition, implying that we do not find sign of a critical end point.

CRediT authorship contribution statement

Szabolcs Borsányi: Conceptualization, Formal analysis, Writing – review & editing; **Zoltán Fodor:** Resources, Funding acquisition, Writing – review & editing; **Jana N. Guenther:** Validation, Writing – review & editing; **Paolo Parotto:** Formal analysis, Validation, Methodology, Writing – review & editing; **Attila Pásztor:** Methodology, Writing – original draft, Writing – review & editing; **Ludovica Pirelli:** Writing – original draft, Conceptualization, Formal analysis, Writing – review & editing; **Kálmán K. Szabó:** Resources, Funding acquisition, Writing – review & editing; **Chik Him Wong:** Software, Writing – review & editing.

Data availability

The authors are unable or have chosen not to specify which data has been used.

Declaration of competing interest

The authors declare that they have no known competing financial interests or personal relationships that could have appeared to influence the work reported in this paper.

Acknowledgments

The project was supported by the BMBF Grant No. 05P21PXFCA. This work is also supported by the MKW NRW under the funding code NW21-024-A. Further funding was received from the DFG under the Project No. 496127839. This work was also supported by the Hungarian National Research, Development and Innovation Office, NKFIH Grant No. KKP126769. This work was also supported by the NKFIH excellence grant TKP2021_NKTA_64. This work is also supported by the Hungarian National Research, Development and Innovation Office under Project No. FK 147164. The authors gratefully acknowledge the Gauss Centre for Supercomputing e.V. (https://www.gauss-centre.eu) for funding this project by providing computing time on the GCS Supercomputer Juwels-Booster at Juelich Supercomputer Centre. We acknowledge the EuroHPC Joint Undertaking for awarding this project access to the EuroHPC supercomputer LUMI, hosted by CSC (Finland) and the LUMI consortium through a EuroHPC Extreme Access call.

References

[1] S. Borsányi, Z. Fodor, J.N. Guenther, R. Kara, P. Parotto, A. Pásztor, L. Pirelli, C.H. Wong, Phys. Rev. D 111 (1) (2025) 14506. https://doi.org/10.1103/PhysRevD.111.014506
[2] A. Bazavov, N. Brambilla, H.T. Ding, P. Petreczky, H.P. Schadler, A. Vairo, J.H. Weber, Phys. Rev. D 93 (11) (2016). Hep-lat, arXiv:1603.06637. https://doi.org/10.1103/PhysRevD.93.114502
[3] A. Adam, S. Borsányi, Z. Fodor, J.N. Guenther, P. Kumar, P. Parotto, A. Pásztor, C.H. Wong, arXiv:2507.13254, 2025 Hep-lat.
[4] S. Borsanyi, Z. Fodor, J.N. Guenther, R. Kara, S.D. Katz, P. Parotto, A. Pasztor, C. Ratti, K.K. Szabo, Phys. Rev. Lett. 125 (5) (2020). Hep-lat, arXiv:2002.02821. https://doi.org/10.1103/PhysRevLett.125.052001
[5] S. Borsanyi, Z. Fodor, J.N. Guenther, P. Parotto, A. Pasztor, L. Pirelli, K.K. Szabo, C.H. Wong, Phys. Rev. D 110 (11) (2024). Hep-lat, arXiv:2410.06216. https://doi.org/10.1103/PhysRevD.110.114507
[6] S. Capitani, S. Durr, C. Hoelbling, JHEP 11, 2006, p.28. arXiv:hep-lat/0607006. https://doi.org/10.1088/1126-6708/2006/11/028
[7] S. Borsanyi, Z. Fodor, J.N. Guenther, S.D. Katz, P. Parotto, A. Pasztor, D. Pesznyak, K.K. Szabo, C.H. Wong, Phys. Rev. D 110 (2024) L011501. Hep-lat, arXiv:2312.07528. https://doi.org/10.1103/PhysRevD.110.L011501
[8] P.J. Gunkel, C.S. Fischer, Phys. Rev. D 104 (5) (2021) 54022. Hep-ph, arXiv:2106.08356. https://doi.org/10.1103/PhysRevD.104.054022
[9] L. Adamczyk, Phys. Rev. C 96 (4) (2017) 44904. Nucl-ex, arXiv:1701.07065. https://doi.org/10.1103/PhysRevC.96.044904
[10] A. Andronic, P. Braun-Munzinger, K. Redlich, J. Stachel, Nature 561 (7723) (2018) 321–330. Nucl-th, arXiv:1710.09425. https://doi.org/10.1038/s41586-018-0491-6